Environmental Health Perspectives
Vol. 61, pp. 307-320, 1985

Quantitative Structure–Activity Relationships of Insecticides and Plant Growth Regulators: Comparative Studies toward Understanding the Molecular Mechanism of Action

by Hajime Iwamura,* Keiichiro Nishimura,* and Toshio Fujita*

Emphasis was put on the comparative quantitative structure–activity approaches to the exploration of action mechanisms of structurally different classes of compounds showing the same type of activity as well as those of the same type of compounds having different actions. Examples were selected from studies performed on insecticides and plant growth regulators, i.e., neurotoxic carbamates, phosphates, pyrethroids and DDT analogs, insect juvenile hormone mimics, and cytokinin agonistic and antagonistic compounds. Similarities and dissimilarities in structures required to elicit activity between compounds classes were revealed in terms of physicochemical parameters, provoking further exploration and evoking insights into the molecular mechanisms of action which may lead to the development of new structures having better qualities.

Introduction

Among various quantitative structure–activity correlation (QSAR) procedures, the Hansch approach has been most widely and effectively used, covering diverse fields of medicinal drugs and agrochemicals (*1–3*). It assumes that the potency of a specified biological activity exerted by a series of compounds can be analyzed by an equation composed of terms of various physiochemical parameters assignable to the structures of the compounds.

Mathematically, the assumption is represented by Eq. (1), using free-energy-related parameters.

$$\log(1/C) = a\pi + \rho\sigma + \delta S + \ldots\ldots + \text{const.} \quad (1)$$

Here, c is the concentration (or dose) of congeneric members that gives a standard response such as EC_{50}, LD_{50}, etc., on a molar basis; π is the hydrophobic substituent parameter defined from oil/water (generally, 1-octanol/water) partition coefficients P as

$$\pi \equiv \log P_x - \log P_H$$

where subscripts denote substituted and unsubstituted compounds (*4*). σ is the Hammett constant for the electronic property of substituents derived from dissociation constants of benzoic acids (*5*). Depending on the situation, the hydrophobicity parameter of the whole molecule, log P, and the electronic parameter for aliphatic substituents such as σ^* (*6*) and σ_I (*7*) can sometimes be used in place of π and σ. S is the steric parameter. According to the mode of steric interactions involved, the Taft E_s (*6,8*), the Verloop STERIMOL (*9*), the van der Waals volume (*10*) or another parameter is used as the steric parameter. In some cases, the squared terms for hydrophobic and steric parameters are required to account for the optima for these effects. Factors for hydrogen bonding (*11*) and parameters for other intramolecular forces such as molecular refractivity (*12*) may be needed in certain cases. By the least-squares method and statistical examinations, the regression coefficients a, ρ, and δ are determined, specifying structural factors contributing to variations in the

*Department of Agricultural Chemistry, Faculty of Agriculture, Kyoto University, Kyoto 606, Japan.

potency. Since the effect of structural variations is separated into components, and significant physiochemical factors are indicated quantitatively, this method may reveal molecular mechanisms involved in processes leading to the elicitation of biological activity. It is especially effective to apply this procedure to the direct comparison of structural requirements for activity between different compound classes showing the same type of activity as well as between the same type of compound classes showing different actions.

In this article, some of our recent QSAR studies on various sets of insecticides and plant growth regulators are reviewed to show the versatility of this procedure not only to elucidate the molecular mechanisms of biological activity but also to examine them by quantitative comparisons.

Insecticides

Antiacetylcholinesterase Phenyl *N*-Methylcarbamates and *O,O*-Dimethylphosphates

Aryl *N*-methylcarbamates and *O,O*-dialkylphosphorothionates are two major groups of compounds to which a number of agricultural insecticides belong, the representative members being carbaryl (I) and fenitrothion (II). The phosphorothionates are usually oxidized *in vivo*,

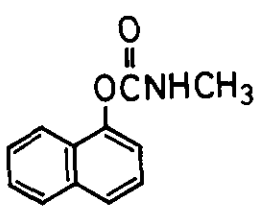

I

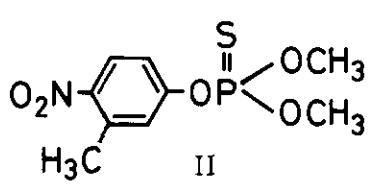

II

giving the corresponding phosphates which are the active principles. Their mode of insecticidal action is well known to be due to inhibition of acetylcholinesterase (AChE). The steps by which these insecticidal esters (ArOX) react with AChE are shown in Equation (2), where EOH denotes the enzyme (*13*).

$$\mathrm{ArOX} + \mathrm{EOH} \underset{k_{-1}}{\overset{k_1}{\rightleftharpoons}} \underset{\text{Complex}}{\text{Reversible}} \xrightarrow{k_2} \mathrm{EOX} + \mathrm{ArOH} \qquad (2)$$

After establishing experimental conditions to determine a reliable set of kinetic parameters $K_d(=k_{-1}/k_1)$ and k_2, for the inhibitory reaction (*14*), the molecular mechanism of enzyme inhibition was extensively investigated. Depending upon the position and nature of substituents, the value of K_d showed significant variations, whereas that of k_2 did not, in each of the carbamates and phosphates. Thus, formation of the reversible complex was considered to be the step which governs the variation in overall inhibitory activity.

Equation (3) is the result of analysis of the K_d (in M) from data obtained using bovine erythrocyte AChE (*15*) for *o*-, *m*- and *p*-substituted phenyl *N*-methylcarbamates (III).

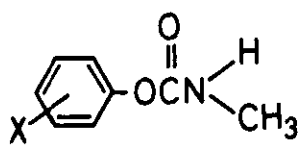

III

$$\begin{aligned}\log(1/K_d) = {} & \underset{(0.168)}{1.399}\pi_{2,3} + \underset{(0.159)}{0.306}\pi_4 + \underset{(0.380)}{1.659}\sigma^{\circ}_{p>0} \\ & - \underset{(0.371)}{1.784}\sigma^{\circ}_{p<0} + \underset{(0.132)}{0.168}E_s + \underset{(0.536)}{0.770}F \\ & + \underset{(0.248)}{1.358}\mathrm{HB} + \underset{(0.162)}{2.592} \qquad (3)\end{aligned}$$

with* $n = 53$
$r = 0.947$
$s = 0.238$

π is derived from the experimentally determined 1-octanol/water partition coefficients, and the subscripts 2,3, and 4 indicate substituents at the *ortho*, *meta*, and *para* positions, respectively. The slopes of the $\pi_{2,3}$ and π_4 terms suggest that the hydrophobic nature of the enzyme surface interacting with the *ortho* and *meta* positions is approximately equivalent, and higher than that of the surface interacting with the *p*-position.

σ° is the electronic parameter which, it is supposed, contains no through-resonance effect (*16*). The effects of *ortho* substituents were treated according to our recently developed procedure (*17,18*) in which the "ordinary" electronic effect of *ortho* substituents was taken as being equivalent to that of *para* substituents. The substituents are classified in terms of electronic effect into two groups: those in one group are more electron withdrawing and promote an attack by a nucleophile of the enzyme on the carbonyl cabon of the carbamyl group, and those in the other group are more electron-releasing and assist an electrophilic attack by an acidic group of the enzyme on the carbonyl oxygen atom. Substituents in the first group are those at the *ortho* position, and those which are electron-withdrawing at the *para* position, such as NO_2, CN, and acyl. Their electronic effect is expressed by the $\sigma^{\circ}_{o>p}$ term. All other substituents belong to the second group, the electronic effect of which

*In this and following equations, n is the number of compounds used in the regression, r is the multiple correlation coefficient and s is the standard deviation. The figures in parentheses are 95% confidence intervals.

is represented by the $\sigma^{\circ}_{o<p}$ term. The significance of these two terms in Equation (3) suggests different mechanisms for the two groups of substituents, leading to a common tetrahedral intermediate as shown in Figure 1. Electron-releasing *ortho* substituents do not follow the negative ρ mechanism because the acid-catalytic site of the enzyme does not fit the carbonyl oxygen atom due to hindrance exerted by these *ortho* substituents.

E_s is the Taft-Kutter-Hansch steric parameter (*8*), the reference of which is shifted to that of H and F is the Swain-Lupton-Hansch field effect constant (*12,19*), both for *ortho* substituents. The coefficient values of these terms, 0.17 and 0.77, are very close to those for the alkaline hydrolysis of *ortho* substituted phenyl acetates (*17*). Thus, in support of the above discussion, the proximity effects of *ortho* substituents are considered to be those on the tetrahedral intermediate formation.

HB, an indicator variable for the hydrogen bonding effect of substituents, is 1 for hydrogen bonding substituents such as *o*-OR, *m*-acyl, -CN, $-NO_2$ and $-NMe_2$, but otherwise is zero. The significance of the term in Equation (3) indicates a specific hydrogen bond formation of these groups with a hydrogen donor on the enzyme. The hydrogen donor site is supposed to be located unsuitably for interaction with other hydrogen bonding groups such as *o*-NO_2, -CN and *m*-OR. Figure 2A shows the stereospecific situation schematically.

The mechanism of the inhibition reaction of the same series of compounds against AChE prepared from fly heads was found to be quite similar to that against bovine erythrocyte AChE [Equation (4)] (*20*).

$$\log(1/K_d) = \underset{(0.212)}{1.554\pi_2} + \underset{(0.143)}{1.134\pi_3} + \underset{(0.134)}{0.238\pi_4} + \underset{(0.279)}{1.147\sigma^{0}_{\rho>0}} - \underset{(0.328)}{1.592\sigma^{\circ}_{\rho<0}} + \underset{(0.168)}{1.188HB_1} + \underset{(0.231)}{0.435HB_2} + \underset{(0.131)}{4.027} \quad (4)$$

with $n = 54$
$r = 0.961$
$s = 0.210$

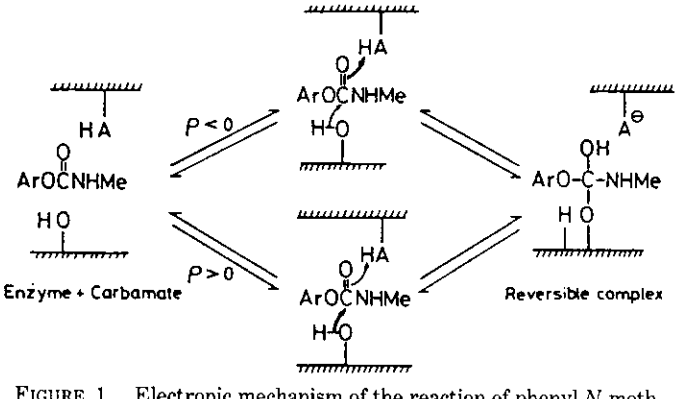

FIGURE 1. Electronic mechanism of the reaction of phenyl *N*-methylcarbamates leading to the tetrahedral intermediate with AChE (*15*). The boldface arrow represents the electron-pair migration occurring as the initiation of the reaction. (Reproduced with permission from Academic Press, Inc.)

One of the slight differences to be noted is that the effect of hydrogen bonding substituents is represented by two indicator variable terms, HB_1 for *o*-OR, -CN, $-NO_2$, *m*-CN, $-NO_2$, and -acyl, and HB_2 for *m*-OR. The hydrogen donor group of fly-head AChE is suggested to be more suitably located for interaction with *m*-OR than that on the bovine erythrocyte AChE as shown in Figure 2B.

Carbamates are metabolically detoxified by a variety of biochemical reactions in the body of the housefly. Among these, the oxidative metabolism generally associated with the mixed-function oxidases has been shown to be of prime importance (*21*). Under conditions where oxidative metabolism was suppressed with piperonyl butoxide, the insecticidal LD_{50} (in mole/head) values against housefly were determined. QSAR analysis gave Equation (5) which resembles Equation (4) for AChE inhibition but the slope of each term is generally lower, suggesting that a detoxification mechanism(s) other than oxidation may be involved in the whole-body activity.

$$\log(1/LD_{50}) = \underset{(0.079)}{0.375\pi_{2,3}} - \underset{(0.079)}{0.082\pi_4} + \underset{(0.390)}{0.995\sigma^{\circ}_{\rho>0}} - \underset{(0.244)}{0.668\sigma^{\circ}_{\rho<0}} + \underset{(0.162)}{0.852HB_1} + \underset{(0.114)}{0.328HB_2} + \underset{(0.074)}{8.419} \quad (5)$$

with $n = 37$
$r = 0.955$
$s = 0.104$

The insecticidal activity values of compounds with strongly electron-withdrawing substituents such as NO_2 and CN are not included in Equation (5). They were considerably lower than those to be expected from their inhibitory activity against AChE, suggesting the possibility of spontaneous hydrolysis during the test period.

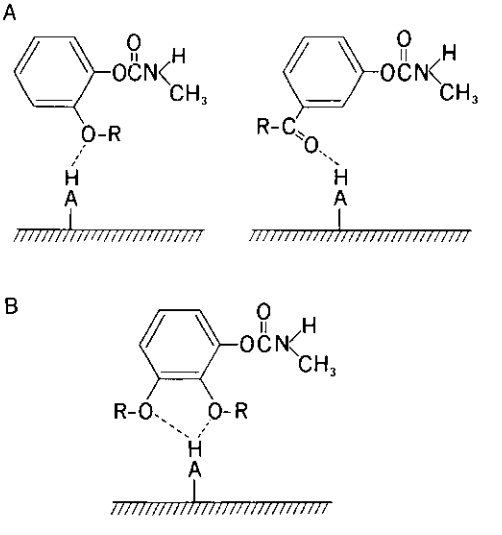

FIGURE 2. Hydrogen bonding formation of phenyl *N*-methylcarbamates with (*A*) bovine erythrocyte (*15*) and (*B*) fly-head AChE (*20*). (Reproduced with permission from Academic Press, Inc.)

These results were helpful in designing new compounds having higher activities. Polysubstituted derivatives having a hydrophobic OR group at the *ortho* position and a hydrophobic alkyl group at the *meta* position were synthesized and, of these, the 2-isopropoxy-5-*n*- and -*s*-butyl derivatives showed high potency as expected (*20*).

The K_d (in M) value for *O,O*-dimethyl- *O*-phenyl phosphates (IV) determined with fly-head AChE was simi-

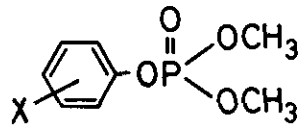

IV

larly analyzed to give Equation (6) (K. Kamoshita and T. Fujita, unpublished data).

$$\log(1/K_d) = \underset{(0.161)}{0.176\pi_{2,3}} + \underset{(0.304)}{2.253\sigma^{\#}} + \underset{(0.215)}{2.892} \qquad (6)$$

$\pi_{2,3}$ is the experimentally determined π value for *ortho* and *meta* substituents. The π term for *para* substituents was not significant in determining the variations in activity. The $\sigma^{\#}$ (sigma mixed) term (*18,22*) is a composite of σ° for *ortho* and *meta* substituents and σ^{-} for *para* substituents (*23*). Since the ρ value (2.25) is close to that in the dissociation of substituted phenols (2.11) (*23*), and also since the σ^{-} is better for the correlation of *para* substituents, the structure of the reversible complex is considered not to be the regular pentacovalent-type but to involve a part of the leaving process of phenoxides as shown in Figure 3.

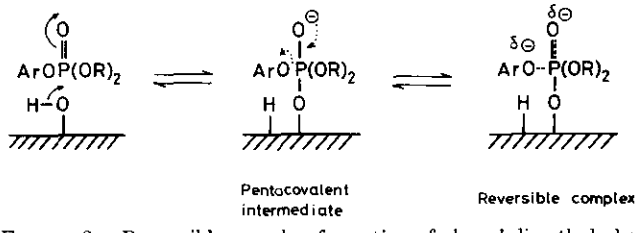

FIGURE 3. Reversible complex formation of phenyl dimethyl phosphates with AChE.

The effect of *ortho* substituents is only the "ordinary" electronic effect as represented by the corresponding σ°(*para*) value, and the proximity factors expressible by F and E_s parameters as in Equation (3) are insignificant. The through-resonance is also insignificant for *ortho* substituents, probably due to the lack of coplanarity of the side chain.

The above QSAR analyses indicate that the detailed substituent effects differ between the two series of compounds. For carbamates, the electronic effect of substituents is position-specific as well as biphasic. Regiospecific hydrophobic and hydrogen-bonding factors operate in addition. For phosphates, the situation is much simpler, complex formation being dependent mostly on the electron-withdrawing substituent effect. We consider these differences to be due in part to the fact that a closer fit into the enzyme is required for the complex formation with carbamates. The core molecular mechanism is, however, common between the two series, being the nucleophilic attack of the serine OH of the enzyme against the ester moiety of insecticides.

Synthetic Pyrethroids and DDT-Related Compounds

The pyrethroids are a class of insecticides from a plant source. Recently, a number of synthetic analogs have been developed that are effective not only against household but also against agricultural pest insects. DDT is a well-known synthetic insecticide. Although its use has been prohibited in a number of countries, the mode of action, as well as structure–activity studies of related compounds, has been continued in the hope of developing analogs devoid of unfavorable environmental impacts.

Although the origins are entirely different, their mode of insecticidal action has been shown to be very similar (*24*). Structural characteristics of compounds have been merged in recently developed novel insecticidal structures as shown in Figure 4 as an example. The principal target site of these two classes of compounds is believed to be the axonal membrane of the nervous system of insects, inhibiting the closing mechanism of the Na^{+} channel (*28,29*). Recently, we have measured the in-

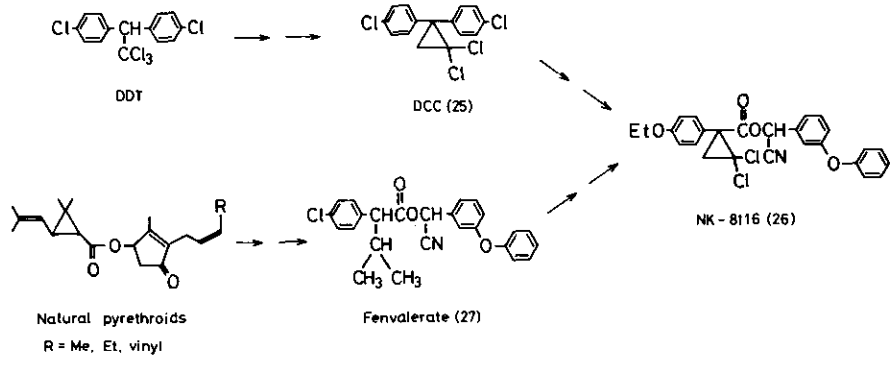

FIGURE 4. Development of a DDT-pyrethroid-hybrid type insecticide.

duction of hyperexcitatory symptoms in excised nerve cords of American cockroaches immersed in physiological saline solution containing various concentrations of substituted-benzyl (+)-*trans*-chrysanthemates (V) and DDT types of compounds (VI–IX) in terms of the min-

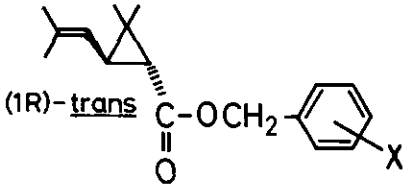

V

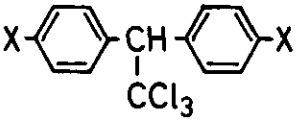

VI

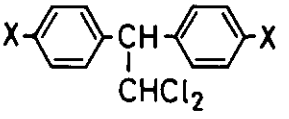

VII

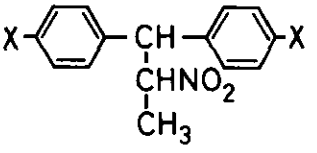

VIII

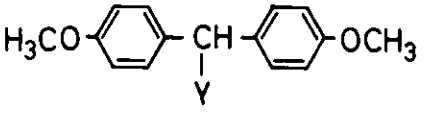

IX

imum concentration (MEC in M) required to induce a repetitive train of impulses in response to a single stimulus (*30*).

The quantitative analysis has been performed for the *ortho*, *meta*, and *para* substituted-benzyl chrysanthemates separately (*31*) to yield Equations (7), (8), and (9). For *ortho* derivatives,

$$\log(1/\mathrm{MEC}) = \underset{(0.673)}{-1.011\sigma} \underset{(0.332)}{- 0.301\pi^2} \underset{(0.332)}{+ 0.405\Delta V_W} + \underset{(0.480)}{5.501} \quad (7)$$

with $n = 14$
$r = 0.878$
$s = 0.372$

For *meta* derivatives,

$$\log(1/\mathrm{MEC}) = \underset{(0.379)}{0.654\Delta V_W} - \underset{(0.066)}{0.066\Delta V_W^2} + \underset{(0.459)}{5.454} \quad (8)$$

with $n = 17$
$r = 0.850$
$s = 0.325$

For *para* derivatives,

$$\log(1/\mathrm{MEC}) = \underset{(0.205)}{-0.344\pi} + \underset{(0.522)}{1.132\Delta V_W} - \underset{(0.098)}{0.260\Delta V_W^2} + \underset{(0.578)}{5.775} \quad (9)$$

with $n = 18$
$r = 0.933$
$s = 0.398$

ΔV_W means the value of van der Waals volume relative to that of H, scaled by 0.1 to make it nearly equiscalar with the other parameters.

Equation (7) indicates that the larger the van der Waals volume, the more favorable are the *ortho* substituents to the excitatory activity on the nerve cords among the substituents tested here. The electron-withdrawing effect of the *ortho* substituents weakens the activity. The activity varies parabolically with the π value, the optimum of which is around $\pi = 0$. Equations (8) and (9) show that the optimum van der Waals volume exists at about 4.9 and 2.2 for *meta* and *para* substituents, respectively. Hydrophobicity of substituents is not favorable to the activity at the *para* position.

In a concentration range higher than those exhibiting repetitive responses, this class of compounds blocks nerve conduction. We have also determined neuroblocking activity in terms of the minimum effective concentration (MBC in M) in the saline solution (*30*). In contrast to the effect on excitatory activity, substituent effects on blocking activity were not specific to substituent positions. With the position-independent hydrophobic and steric parameters, Equation (10) was formulated for 20 benzyl chrysanthemates where definite activity indices are available (*31*).

$$\log(1/\mathrm{MBC}) = \underset{(0.138)}{0.370\Delta V_W} - \underset{(0.158)}{0.283\pi^2} + \underset{(0.240)}{3.972} \quad (10)$$

with $n = 20$
$r = 0.284$
$s = 0.812$

Peculiar "topographical" effects of substituents have long been observed for toxicity of substituted-benzyl chrysanthemates against houseflies (*32*). The effect of the benzyl group attached to the benzyl ring is highest in the *meta* while lowest in the *ortho* derivative. For the allyl derivatives, activity was highest in the *para* and lowest in the *ortho* isomer. Equations (7)–(9) indicate that the optimum van der Waals volume of substituents for the neuroexcitatory activity is largest at the *ortho* and smallest at the *para* position. In Figure

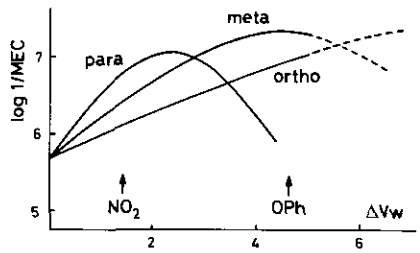

FIGURE 5. Position-dependent steric effect on the neuroexcitatory activity of substituted benzyl (1R)-*trans*-chrysanthemates (*31*). (Reproduced with permission from Academic Press, Inc.)

5, the activity is expressed as the function of the ΔV_W value at each position according to Equations (7)–(9). It is easily understood that, other factors being equal, the sequence of the activity among positional isomers varies from *para* > *meta* > *ortho via meta* > *para* > *ortho* to *meta* > *ortho* > *para* with increase in the bulkiness of substituent from nitro to phenoxy. Since the neurobblocking activity is not position-specific, the peculiar topographic effects of substituents on the insecticidal activity of benzyl chrysanthemates are understood on the basis of those on the neuroexcitatory activity.

For the aromatic substituent effects on the neuroexcitatory activity of DDT (VI), DDD (VII), prolan (VIII), and their analogs, Equation (11) was formulated (*33*), where I is an indicator variable for prolan:*

$$\log(1/\mathrm{MEC}) = \underset{(0.411)}{2.744}\Delta V_W - \underset{(0.124)}{0.665}\Delta V_W^2 + \underset{(0.287)}{0.469}I + \underset{(0.322)}{4.816} \quad (11)$$

with $n = 25$
$r = 0.957$
$s = 0.292$

analogs. There is practically no difference in activity between the DDT and DDD series if the aromatic substituents are the same. The optimum ΔV_W value is about 2.1, which is close to those of Et and OEt. This optimum is very similar to the value for the *para* substituent effect of benzyl (+)-*trans*-chrysanthemates on the same type of activity. The aromatic moiety of the pyrethroids and DDT-type compounds may fit into the target sites at the axonal membrane with a closely related (or a common) mechanism.

For the effect of benzylic substituents examined with the methoxychlor analogs (*IX*), Equation (12) was formulated (*33*), where L is the STERIMOL length parameter (*9*).

$$\log(1/\mathrm{MEC}) = \underset{(1.426)}{2.987}\Delta V_W - \underset{(0.199)}{0.217}\Delta V_W^2 - \underset{(0.392)}{1.121}L - \underset{(0.142)}{0.511}\pi^2 - \underset{(2.792)}{4.480} \quad (12)$$

with $n = 17$
$r = 0.961$
$s = 0.409$

Equation (12) reveals that the optimum bulkiness and the optimum hydrophobicity of substituents are located at about $\Delta V_W = 6.89$ and $\pi = 0$, respectively. Equation (12) also shows that the shorter the length of benzylic substituents, the higher is the activity. Thus, thickset substituents are desirable for high activity. Although the requirements for the optimum bulkiness as well as for the optimum length are not satisfied simultaneously, such thickset substituents as CBr_3, $CH(Et)NO_2$, and $C(Me)_2NO_2$ are in fact most favorable.

Holan proposed that benzylic substituents of DDT analogs would fit into the channel of a pore in the cell membrane to induce leakage of Na^+ ion (*34*). He demonstrated that the optimum diameter of the benzylic substituents is about 6 to 6.3 Å to plug the pore. Assuming the substituent with 6 to 6.3 Å diameter to be a sphere, the volume is calculated as being about 73 cm^3/mole, which is very close to the optimum van der Waals volume estimated from Equation (12), which is about 72.5(= [optimum ΔV_W + V_W (H)] × 10).

Equation (13) was derived for the insecticidal activity against the American cockroach in terms of the minimum lethal dose (MLD in mole/insect) of four series of DDT-type compounds where definite activity was determinable by injection (*33*).

$$\log(1/\mathrm{MLD}) = \underset{(0.144)}{0.531}\log(1/\mathrm{MEC}) + \underset{(0.122)}{0.169}\log P + \underset{(1.196)}{3.013} \quad (13)$$

with $n = 31$
$r = 0.839$
$s = 0.305$

The insecticidal activity is determined by the neuroexcitatory activity when the role of hydrophobicity (log P) in the transport process to the target was considered and separated.

The above analyses indicate a number of similarities in structure–activity relationships, in particular, in parabolic dependencies of neuroexcitatory activity on steric factors between two series of compounds. They are, however, still incomplete, and the accumulation of this type of analyses systematically performed for a number of substructural features would be one of the most rational approaches in comparing the molecular mechanism of actions.

Insect Juvenile Hormone Mimics

Insect juvenile hormone (JH) mimetic compounds are divided roughly into two classes, terpenoid and nonterpenoid types. A representative of the first class, isopropyl (2E, 4E)-11-methoxy-3,7,11-trimethyl-2,4-dodecadienoate, named methoprene (X), exhibits high

*Equations (11) and (12) vary slightly from the original ones (*33*), where some of the data were erroneously used.

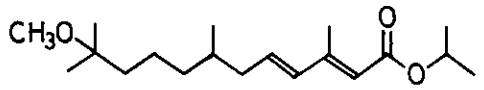

X

activity on *Aedes aegypti* (yellow-fever mosquito) but it is not always so on other insect species (*35*). For *Tenebrio molitor* (yellow mealworm), the most active member is *N*-ethylamide of dodecadienoic acid (XI) (*36*). *N*-Ethyl-1,2-bis(isobutylthiolcarbamoyl)ethane (XII)

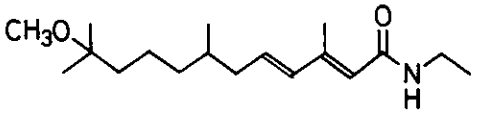

XI

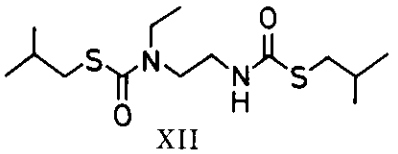

XII

belongs to the nonterpenoid class and possesses outstanding activity on *T. molitor* (*36*), and *N*-[4-(3-chlorobenzyloxy)benzyl]-2,6-difluoroaniline (XIII), a

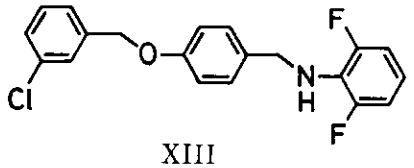

XIII

compound of high aromatic content, shows a moderate activity on the same insects (*37*). The compounds in the nonterpenoid class are not always very active but are novel in structure. It is expected that they provide possibilities to develop useful compounds without the deficiencies like poor field stability and costly synthesis of the compounds having integrity of the terpenoid structure.

2,4-Dodecadienoates and related compounds are a class having the highest total number of compounds tested so far for activity. Using the data published by Henrick et al. (*38*), analyses were performed for activities on *A. aegypti* and *T. molitor*, quantitatively in terms of physicochemical parameters, to explore the similarities as well as dissimilarities between the species of the structural effects on activity (*39*). The structural information obtained could be transposed to other, nonterpenoid types of compounds if the site of action or the receptor is the same.

The structure of the series of compounds shown in Figure 6 varies at both ends, X and Y, of the chain. To express the molecular shape, the steric parameters shown by Figure 7 were defined. L_x is the length of the X end along the bond axis (C_1-X), and W_x is the width in the direction in which the longest chain of the X substituents extends in the staggered conformation. The maximum length of the whole molecule was expressed by the D parameter, which is the summation of the D_x and D_y. The D_x is the length of the X moiety along an axis which passes through the C_1 and C_{11} atoms in the fully extended conformation and the D_y is that of the Y moiety. The D parameter is accordingly the length of the molecule after the common C_1–C_{11} part is subtracted. The B_x parameter shown by Figure 8 manifests the bulkiness toward the carbonyl group of α-substituents in the alcohol moiety of ester and thiolester derivatives. The values of these steric parameters are calculated geometrically based on the CPK models using the STERIMOL program (*9*).

The hydrophobicity of the X end, π_x, is expressed by the π value of the C(Me) = CH-CO-X moiety, taking the conjugation of X with the α,β-unsaturated carbonyl group into consideration. The π_y term is the hydrophobicity of the Y-C_{11}–C_{10} moiety since some compounds have substituents at the A and/or B positions defined in Figure 6.

After separate analyses for two sets of compounds where either the X or Y end is held constant, Equation

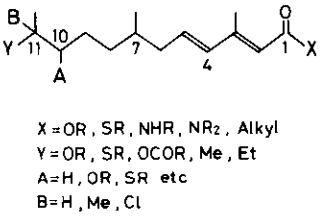

FIGURE 6. Structure of JH-mimetic 2,4-dodecadienone derivatives (*39*). (Reproduced with permission from the American Chemical Society.)

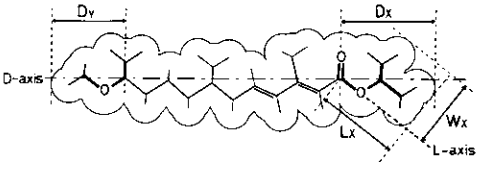

FIGURE 7. Schematic representation of the steric parameters (*39*). The ends of the bars of the model represent hydrogen atoms. (Reproduced with permission from the American Chemical Society.)

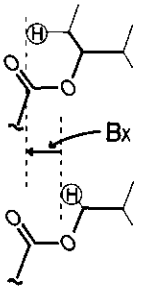

FIGURE 8. Schematic representation of the steric B_x parameter for esters (*39*). (Reproduced with permission from the American Chemical Society.)

(14) for *A. aegypti* and Equation (15) for *T. molitor* were derived for the combined set with the whole-molecular as well as the substructural parameters.
For *A. aegypti:*

$$\begin{aligned} pI_{50} = {} & \underset{(1.26)}{3.65L_x} - \underset{(0.11)}{0.35L_x^2} + \underset{(1.12)}{1.08D^2} \\ & - \underset{(0.06)}{0.06D^2} + \underset{(1.13)}{1.90 \log P} - \underset{(0.09)}{0.14(\log P)^2} \\ & + \underset{(0.25)}{0.57B_x} - \underset{(0.41)}{0.71I_N} + \underset{(0.35)}{0.86I_{OR}} \\ & - \underset{(0.65)}{1.39I_{br}} - \underset{(0.37)}{0.65I_{(-)}} - \underset{(5.21)}{16.35} \end{aligned} \quad (14)$$

with $n = 85$
$r = 0.89$
$s = 0.53$

For *T. molitor*:

$$\begin{aligned} pI_{50} = {} & \underset{(1.69)}{4.63W_x} - \underset{(0.21)}{2.58W_x^2} + \underset{(1.14)}{2.58D^2} \\ & - \underset{(0.06)}{0.15D^2} + \underset{(1.13)}{1.76 \log P} - \underset{(0.09)}{0.13(\log P)^2} \\ & + \underset{(0.30)}{0.61\pi_x} + \underset{(0.26)}{0.87B_x} + \underset{(0.47)}{2.89I_{NR}} \\ & - \underset{(0.71)}{2.51I_{br}} - \underset{(5.96)}{23.32} \end{aligned} \quad (15)$$

with $n = 84$
$r = 0.90$
$s = 0.54$

pI_{50} is the logarithm of reciprocal of the I_{50} value, which is the molar concentration for *A. aegypti* larva and mole/pupa for *T. molitor* to produce 50% inhibition of metamorphosis.

Significance as well as the overlaps of the coefficient values of the log P and its squared term in Equations (14) and (15) indicate the similarity of the transport processes. Other common terms are D, B_x, and I_{br}. I_{br} is an indicator variable for compounds having a branch at any position in the X moiety of ketone derivatives. Its negative coefficient may suggest that the branch obstructs the proper fit in the receptor. Contrary to this, the branch parameter of esters, B_x, has a positive coefficient. The esters appear susceptible to hydrolysis, and the site of the enzymatic attack of those having an α-branch becomes sterically hindered. It is interesting that the D term, which is the summation of D_x and D_y, is significant. This suggests that the X and Y ends are located at the site of action parallel in terms of the D_x and D_y axes, irrespective of the conformation of the middle part of the molecule. On this basis and minimizing the strains between bonds, a model-building study suggested an extended active conformation like that depicted by Figure 7.

An important factor in determining the activity is the length of the X-substituents, L_x in Equation (14) for *A. aegypti*, whereas it is the width parameter W_x in Equation (15) for *T. molitor*. The significance of the squared terms suggests that a receptor wall exists in the L_x direction ca. 5 Å, the optimum value, distant from the C_1 atom in the *A. aegypti* receptor and it is located in the W_x direction ca 3.8 Å distant from the L_x axis in the *T. molitor* receptor. The L_y and W_y parameters derived similarly to L_x and W_x were found to be insignificant, showing receptor wall existing only in the direction of the D_y axis at the Y end. For the C_7 enantiomeric effect, the (R)-(−)-isomer always shows lower activity in *A. aegypti* than the (±)-counterpart. A spatial wall is thought to exist closer to the methyl group at the C_7 atom in the interaction site, and this is expressed by the indicator variable term $I(-)$, which takes the value of 1.0 for the (R)-(−)- and zero for the (±)-isomer. Another term which reflects the species difference is the position-specific π_x term in Equation (15). The region of the *T. molitor* receptor with which the X moiety is in contact is considered to be hydrophobic in nature, and interacts more strongly with compounds having a hydrophobic X moiety.

The I_{NR} is an indicator variable that takes the value of 1.0 for the amides and ketones and is otherwise zero. Its significance with the positive sign in Equation (15) for *T. molitor* may reflect the resistance of the amides to and the impotency of the ketones against hydrolytic attack by the enzyme. The insignificance of the I_{NR} term in Equation (14) seems to reflect the weaker potency of *A. aegypti* hydrolytic enzyme. The I_N in Equation (14) is an indicator variable that takes 1.0 for amides and

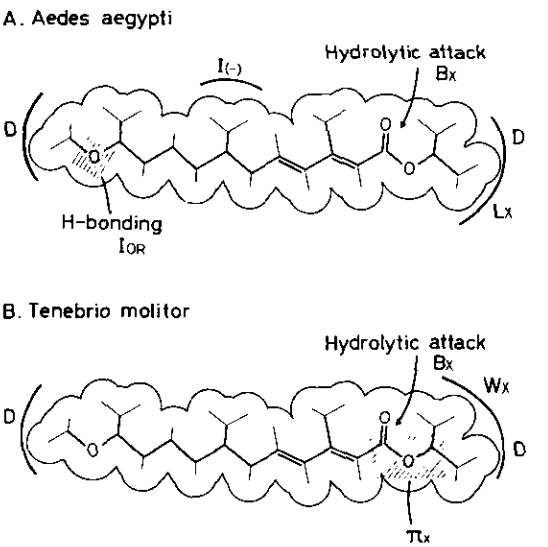

FIGURE 9. Binding models of 2,4-dodecadienoates to (*A*) *A. aegypti* and (*B*) *T. molitor* receptors (*39*). The solid lines are the steric interaction sites or spatial walls. The region indicated by oblique lines in *A* is the H-bonding site and that in *B* is the hydrophobic interaction site. The arrows directed toward the carbonyl group indicates the possible hydrolytic site. The affixes are the parameters incorporated into Eqs. (14) and (15) to suggest these sites. The compound used in the model is methoprene (X). (Reproduced with permission from the American Chemical Society.)

zero for the others. Its physicochemical meaning is obscure but the negative coefficient shows that the activity of amides is uniformly lower in *A. aegypti*. Another indicator variable term I_{OR} in Equation (14) takes 1.0 for the compounds whose Y moiety is alkoxy and otherwise zero. This effect seems to be due to a hydrogen-bonding type interaction with an acidic group on the receptor, enhancing binding. With a most favorable combination of various factors, the very potent activity of isopropyl 11-methoxy-3,7,11-trimethyl-2,4-dodecadienoate(methoprene X) on *A. aegypti* and that of the corresponding *N*-ethylamide (XI) on *T. molitor* are understandable.

Based on these results, an inclusive "mode of action" map was drawn and shown in Figure 9*A* for *A. aegypti* and 9*B* for *T. molitor*. The affixes explain the roles or meanings of the parameters incorporated into the correlations. The models help in understanding the overall resemblance as well as the species difference of the mode of action.

It is worthwhile to test the validity of the receptor models and/or the possibility of transposing the structural information to other classes of compounds. Thus, in Figure 10*A*, the CPK model of the nonterpenoid *N*-ethyl-1,2-bis(isobutylthiolcarbamoyl)ethane (XII) was accommodated to a model which shows inclusively the receptor contour of both insect species with that of methoprene. The carbamoylethane that fits well into the model reportedly exhibits a high morphogenetic activity on *T. molitor* (*36*), but the activity data on *A. aegypti* is lacking. The compound is expected to show some activity on *A. aegypti*, if the *N*-ethyl group does not interact so badly with the $I(-)$ wall. Figure 10*B* is the result on *N*-[4-(3-chlorobenzyloxy)benzyl]-2,6-difluoroaniline (XIII), which possesses a seemingly very different structure and exhibits, although moderately, activity on *T. molitor* (*37*). It has a conformationally rigid benzene ring at the center of the molecule. If one assumes the same target site, both ends should be parallel, and thus an extended conformation as shown by Figure 10*B* is adopted.

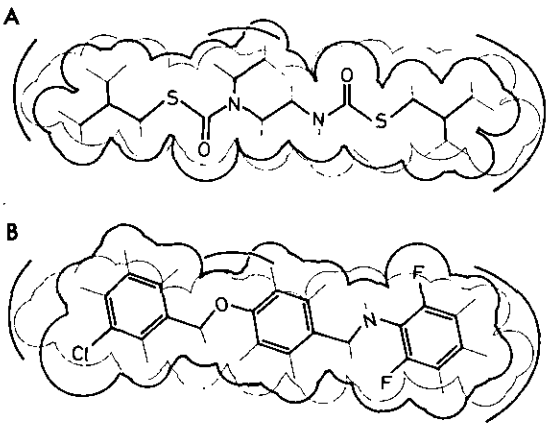

FIGURE 10. Comparison of the molecular shape of non-terpenoid JH-mimetic compounds with that of terpenoid type, methoprene (X) (*39*): (*A*) compound XII; (*B*) Compound XIII. The thick solid line represents the contours of the CPK models of these compounds and the thin solid line that of methoprene. The spatial walls of the *A. aegypti* and *T. molitor* receptors are also shown inclusively by the solid line. (Reproduced with permission from the American Chemical Society.)

The approaches could be extended to other insect species as well as to other diverse classes of compounds. In these phases, the mode of action models or the receptor maps will act as a guide. Over the dissimilarities of the modes of action between species, the structural essentials which confer the JH activity through species would be more clearly indicated.

Plant Growth Regulators

Cytokinin-Active Adenine and Urea Derivatives

The term cytokinin refers to a class of plant hormones that promote cell division and growth in certain plant tissues. They are often involved in cell differentiation and organ formation, enhancement of seed germination, and resistance to senescence. 6-[(E)-4-Hydroxy-3-methyl-2-butenylamino]purine(zeatin) and 6-(3-methyl-2-butenylamino)purine are naturally occurring representatives of this class. *N,N'*-Diphenylurea, isolated as a cell-division factor of coconut milk (*40*), is in another class of cytokinins which possess seemingly very different structures from but the same activity as the N^6-substituted adenines.

With the aim of elucidating structure–activity relationships as well as at developing highly active analogs, a large number of related compounds have been synthesized in both series of cytokinins. To reveal the correspondence of structural requirements between two series of compounds, the QSAR technique has been utilized (*41*). Equation (*16*) was formulated for a number of N^6-alkyl- and N^6-substituted benzyladenines (XIV).

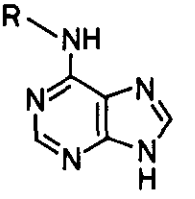

R: Alkyl or substituted benzyl

XIV

Equation (17) was derived from the data determined by Bruce and Zwar (*42*) for *N,N'*-diphenylureas having substituents on one of the benzene rings (XV).

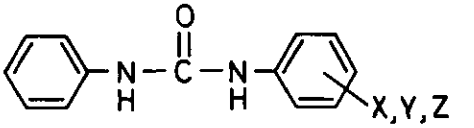

XV

For N^6-substituted adenines:

$$\log(1/E_{50}) = \underset{(1.71)}{3.35W_{max}} - \underset{(0.15)}{0.32(W_{max})^2} - \underset{(0.26)}{0.65W_{o,m}} + \underset{(0.98)}{2.03\sigma^*} - \underset{(4.74)}{1.50} \quad (16)$$

with $n = 22$
$r = 0.85$
$s = 0.26$

For N,N'-diphenylureas:

$$\log(1/C) = \underset{(0.33)}{0.90\sigma} - \underset{(0.25)}{0.85L_o} - \underset{(0.22)}{0.27L_p} + \underset{(0.58)}{1.04\pi_m} + \underset{(0.32)}{5.00} \quad (17)$$

with $n = 39$
$r = 0.91$
$s = 0.38$

E_{50} in Equation (16) is the molar concentration at which the 50% of the maximum callus yield is obtained in the tobacco callus bioassay, and C in Equation (17) is the minimum molar concentration at which the activity is detected in the tobacco pith assay. W_{max} is the maximum width perpendicular to the bond axis of the N^6-substituents, as shown in Figure 11. Since the bulkiness of *ortho* and *meta* substituents on the N^6-benzyl moiety is not reflected by the W_{max} parameter as depicted by Figure 12, their "maximum" width was separately defined as $W_{o,m}$. L_o and L_p are the length parameters for *ortho* and *para* substituents of diphenylureas and π_m is the hydrophobic parameter of the *meta* substituents. W and L parameters were calculated by the STERIMOL program (*9*) for the fully extended conformation.

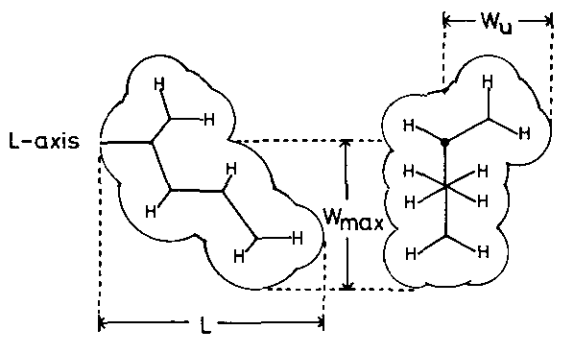

FIGURE 11. Schematic representation of the steric W parameters (*50*). (Reproduced with permission from the American Chemical Society).

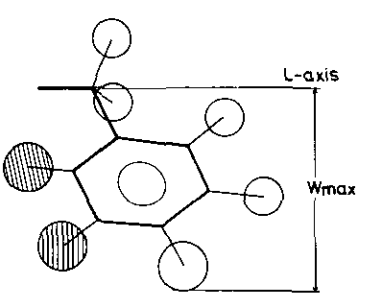

FIGURE 12. Schematic representation of the steric W_{max} parameter of the benzyl moiety (*41*). The maximum width of the shadowed *m*- and *p*-substituents entered into Eq.(17). (Reproduced with permission from Pergamon Press, Ltd.)

The significance of the $(W_{max})^2$ term in Equation (16) shows that there is an optimum steric condition (ca. 5.2 Å) for activity in terms of the maximum width at the N^6-substituents of adenylate cytokinins. The negative coefficient of the $W_{o,m}$ term indicates that, the thicker the *ortho* and *meta* substituents, the lower the activity. For N,N'-diphenylurea derivatives, Equation (17) indicates that the position-specific steric and hydrophobic effects of the aromatic substituents are of major importance in determining the activity. At the *ortho* and *para* positions, substituents length is unfavorable, as shown by their negative coefficient. No particular length effect is observed for *meta* substituents, but their high hydrophobicity enhances activity. The hydrophobicity of the whole molecule is, however, not significant in both series, suggesting that transport in the tobacco tissue is not a process important for activity within the compound sets analyzed. Variations in activity are thus governed mainly by variations in the interaction with the target site.

The electron-withdrawing effect expressed by the positive sign of the Taft's σ^* term in Equation (16) for N^6-substituents of adenines is considered to be operative at the N^6-H. A similar electronic effect indicated by the Hammett σ term in Equation (17) suggests an electronic interaction via the NH group on the urea bridge. The basic partner group of the interaction could be common with that for the adenylate cytokinins, if one assumes the same receptor. The site of interaction for the substituted benzene moiety of diphenylureas is then better considered to correspond to the heterocyclic moiety of the adenylate cytokinins, since the position-specific hydrophobic effect expressed by the π_m term is not observed for the N^6-substituents in adenine derivatives.

On the basis of these results, the modes of binding for both the adenine and urea cytokinins to the site(s) of action are schematically represented in Figure 13. The stippled lines in the figure represent the steric interaction sites or the spatial walls deduced from the steric parameters incorporated into Equations (16) and (17), and the smooth line facing the NH groups is the electron-donating site. The striped circle is the hydrophobic region where the *meta* substituents of the diphenylureas come on when they fit with the receptor, as suggested by the π_m term in Equation (17). The combined binding model displays the structural correspondence and/or similarity between the two series of cytokinins. Since the identity of their sites of action has recently been indicated by a kinetic approach (*43*), Figure 13 is considered to show the physicochemical entity of cytokinin receptor as well, the results from the two series of compounds complementing each other.

Cytokinin-Agonistic and Antagonistic Pyrrolo[2,3-d]pyrimidines

Antagonists of a biologically active compound play an important role in studying its bioregulatory mechanisms and mode of action. In this respect, quite a few structural classes of cytokinin antagonists, anticytokinins, have been developed recently (*44–48*), all of which possess similarities in structure to N^6-substituted adenylate cytokinins. Among these, N^4-substituted 4-amino-2-methylpyrrolo[2,3-d]pyrimidines (XVI) are unique

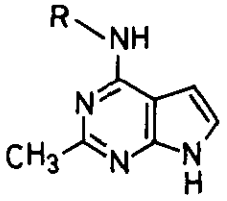

R: Alkyl or substituted phenyl

XVI

since their activity varies from agonistic to antagonistic with the transformation of the N^4-side chain (*47*). They are accordingly a class of compounds structurally congeneric but having different types of activity.

The identity of their receptor has been shown kinetically by the method of Lineweaver and Burk (*49*), where the reciprocal of the growth response in terms of the tobacco callus yield was plotted against the reciprocal of the concentration of added cytokinin (*50*). Figure 14 shows an example for an antagonistic cyclopentyl derivative, where the family of straight lines possesses a common intercept, fulfilling the requisite for competitive inhibition. The question that immediately arises is how their interaction with the common receptor leads to different biological results.

Both N^4-alkyl and N^4-phenyl derivatives exhibit activity, agonistic or antagonistic depending on the structure. The steric features were thought to be responsible for the activity change, the maximum width (W_{max}) and the thickness (W_n) upward and rectangular to the W_{max}, being most plausible. The definition of steric parameters are shown in Figure 11. Equation (18) is the one finally correlated for the combined set of compounds.

$$\log(1/A) = \underset{(1.86)}{2.98W^{R}_{max}} - \underset{(0.19)}{0.33(W^{R}_{max})^2} + \underset{(0.37)}{1.10W^{R}_{n}} - \underset{(0.26)}{0.35L^{R}} - \underset{(0.27)}{1.09W^{Ph}_{max}} + \underset{(4.64)}{10.25I^{Ph}_{n}} + \underset{(0.65)}{1.21\sigma^{*}} + \underset{(0.15)}{0.53\pi} - \underset{(4.53)}{8.27} \quad (18)$$

with $n = 44$
$r = 0.92$
$s = 0.39$

The A expresses E_{50}, the molar concentration required for 50% of the maximum growth of the tobacco callus, when compounds are agonistic and, when antagonistic, it is I_{50}, the molar concentration required for 50% inhibition of callus growth promoted by kinetin. The steric parameters for the alkyl series of compounds were separated to be significant from those for the phenyl series of compounds. Those for the alkyl series are marked by a superscript R and those for the latter by Ph. This result means that the exact mode of steric interactions with receptor is different between the two series, reflecting the different substituent shapes. In phenyl derivatives, it is governed by the maximum width, W^{Ph}_{max}, and, in alkyl derivatives, by W^{R}_{max}, W^{R}_{n}, and L^{R}. The significance of the $(W^{Ph}_{max})^2$ term indicates that there is an optimum steric condition for the binding of the alkyl derivatives. The predicted optimum value, 4.7 Å, coincides with the value, 4.2 Å, estimated for the N^6-

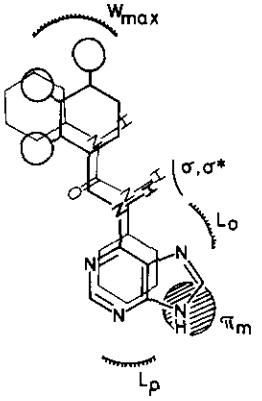

FIGURE 13. Cytokinin-receptor binding model showing the structural correspondence between adenine and urea derivatives (*41*). Models used are N^6-benzyladenine and diphenylurea. A hexagon represents the benzene ring. Stippled lines show the spatial walls, the smooth line the electron-donating site, and the striped circle the hydrophobic region. (Reproduced with permission from Pergamon Press, Ltd.)

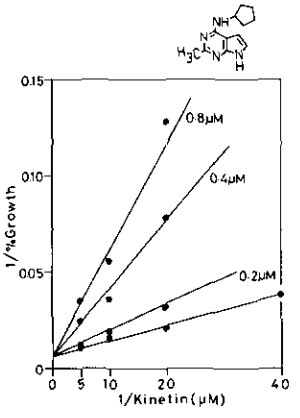

FIGURE 14. The Lineweaver and Burk plots for the antagonistic nature of the indicated compound to kinetin (*50*). The ordinate expresses the reciprocal of the growth rate of tobacco callus in the absence (bottom line) and in the presence of the compound in various concentrations as indicated. (Reproduced with permission from the American Chemical Society.)

adenylate cytokinins in the preceding section, providing us with an insight into the bulkiness of the receptor cavity into which the alkyl substituents must fit. The I_n^{Ph} is an indicator variable for phenyl derivatives. Its significance means that a factor which uniformly enhances activity of the aromatic congeners is operating, although its physicochemical basis is unknown but probably due to the difference of the substituent shape.

The electronic and hydrophobic factors are common through both the agonists and antagonists. The σ^* term is suggestive of an electronic interaction at the common N^4-imino hydrogen atom with a basic site on the receptor surface. The antagonists presumably scramble for the site with agonists. Another common term, π^*, with positive coefficients, shows the importance of hydrophobicity, probably in the transport process.

Equation (18) explains the potency of activity irrespective of the quality of activity, agonistic or antagonistic. Figure 15 shows the parabolic dependence of the cytokinin agonistic and antagonistic activities of alkyl derivatives on the W_{max}^R value, and Figure 16 the linear, downward relationship of the activity of phenyl derivatives to W_{max}^{Ph}. Conspicuous is the fact that the W_{max}^R values of alkyl derivatives having agonistic activity and denoted by open circles are in the range of 4.5–6.0 Å and the compounds having the W_{max}^R values outside this range are anticytokinins. At the same time, they are on the common parabolic curve in terms of W_{max}^R. The results coincide with and provide evidence for the hypothetical concept for hormonal action that agonist binding causes a conformational change of an otherwise inactive receptor to the active form and that antagonists are species that bind similarly to the receptor but do not cause the effective conformational change. In the present case, the interaction at the W_{max}^R region is responsible not only for the binding but also for the quality of activity, i.e., a conformational change leading to the active species. The interaction at the W_{max}^{Ph} region has the same role also in the phenyl series of compounds, the agonists having the values larger than ca. 4.0 ÅA.

Within the congeneric phenyl derivatives, Equation (18) indicates that compounds having as large as possible π and σ^* values and as small as possible W_{max}^{Ph} values should be highly active as anticytokinins. The *p*-CF_3 and *p*-i-Pr derivatives, the highest active members of the class, were thus derived.

Concluding Remarks

The above examples show that much invaluable information has been derived from quantitative comparisons of physicochemical factors determining structure–activity relationships. As stated earlier in this article, they are broadly classified into two types. In the first type, the comparisons were made between different classes of compounds having the same type of activity such as antiacetylcholinesterase carbamates vs. phosphates, pyrethroids vs. DDT-related compounds and adenylate vs. diphenylurea cytokinins. In the second type, structural factors were compared within a single type of compound; between subsets of a series of N^4-substituted pyrrolopyrimidines exhibiting cytokinin-agonistic and antagonistic actions and between activities against different insect species of a series of dodecadienoate juvenoids. In each example, similarities and dissimilarities in molecular mechanisms of action between counterparts were clearly demonstrated. Accumulation of QSAR results within each comparative study is expected to lead to the revelation of novel empirical rules determining structure–activity relationships as well as to reinforcing the validity of molecular mechanisms.

The information obtained from the QSAR analyses is helpful in designing compounds of optimized structure having the most favorable activity by modifications of

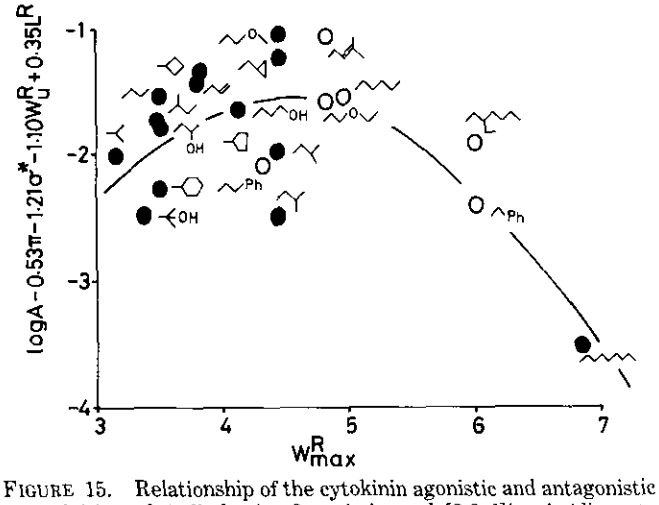

FIGURE 15. Relationship of the cytokinin agonistic and antagonistic activities of 4-alkylamino-2-methylpyrrolo[2,3-d]'pyrimidines to W_{max} as expressed by Eq. (18) (*50*). The compounds denoted by open circles are those having agonistic activity. (Reproduced with permission from the American Chemical Society).

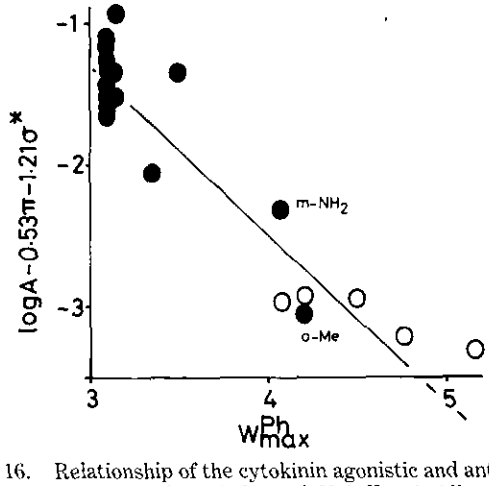

FIGURE 16. Relationship of the cytokinin agonistic and antagonistic activities of 4-anilino-2-methylpyrrolo[2,3-d]pyrimidines to W_{max} expressed by Eq. (18) (*50*). The compounds denoted by open circles are those having agonistic activity. (Reproduced with permission from the American Chemical Society.)

substructures. In fact, a number of attempts have been made to apply this procedure to structural optimization to derive useful bioactive compounds with varying degrees of success (*3,51–55*). The comparative QSAR studies not only promote such structural optimization procedures but are also useful in providing indications for developing other classes of compounds showing the same type of activity and having novel structural features, by integrating empirical rules governing structure–activity profiles. In cases where molecular shape is important, the "receptor-contour-maps" may be of use.

The examples in this article were selected only from the areas of insecticides and plant growth regulators. Similar comparative QSAR studies for different compound series having the same type of activity have also been performed in other fields of pesticides which include agricultural fungicides (*56*) and photosynthesis-inhibitory herbicides (*57*). Recently, this type of QSAR analysis has been applied to environmental toxicological problems (*58*). We hope that comparative studies could also be accumulated for environmental problems so that the Hansch approach would integrate the methodologies for structure–property relationships which have been carried out independently in the field of drug and pesticide pharmacology and in the field of environmental toxicology.

REFERENCES

1. Hansch, C., and Fujita, T. ρ-σ-π analysis. A method for the correlation of biological activity and chemical structure. J. Am. Chem. Soc. 86: 1616–1626 (1964).
2. Hansch, C. On the structure of medicinal chemistry. J. Med. Chem. 19: 1–6 (1976).
3. Topliss, J., Ed. Quantitative Structure-Activity Relationships of Drugs. Academic Press, New York, 1983, pp. 1–519.
4. Fujita, T., Iwasa, J., and Hansch, C. A new substituent constant, pi, derived from partition coefficients. J. Am. Chem. Soc. 86: 5175–5180 (1964).
5. Hammett, L. P. Physical Organic Chemistry, 2nd ed. McGraw-Hill, New York, 1970, pp. 347–390.
6. Taft, R. W. Separation of polar, steric, and resonance effects in reactivity. In: Steric Effects in Organic Chemistry (M. S. Newman, Ed.), John Wiley, New York, 1956, pp. 556–676.
7. Charton, M. Electrical effect substituent constants for correlation analysis. In: Progress in Physical Organic Chemistry, Vol. 13 (R. W. Taft, Ed.), John Wiley, New York, 1981, pp. 119–252.
8. Kutter, E., and Hansch, C. Steric parameters in drug design. Monoamine oxidase inhibitors and antihistamines. J. Med. Chem. 12: 647–652 (1969).
9. Verloop, A., Hogenstraaten, W., and Tipker, J. Development and application of new steric substituent parameters in drug design. In: Drug Design, Vol. 7 (E. J. Ariëns, Ed.), Academic Press, New York, 1976, pp. 165–208.
10. Bondi, A. Van der Waals volume and radii. J. Phys. Chem. 68: 441–451 (1964).
11. Fujita, T., Nishioka, T., and Nakajima, M. Hydrogen-bonding parameter and its significance in quantitative structure–activity studies. J. Med. Chem. 20: 1071–1081 (1977).
12. Hansch, C., Leo, A., Unger, S. H., Kim, K. H., Nikaitani, D., and Lien, E. J. Aromatic substituent constants for structure-activity correlations. J. Med. Chem. 16: 1207–1216 (1973).
13. Wilson, I. B., Harrison, M. A., and Ginsburg, S. Carbamyl derivatives of acetylcholinesterase. J. Biol. Chem. 236: 1498–1500 (1961).
14. Nishioka, T., Kitamura, K., Fujita, T., and Nakajima, M. Kinetic constants for the inhibition of acetylcholinesterase by phenyl carbamates. Pestic. Biochem. Physiol. 6: 320–327 (1976).
15. Nishioka, T., Fujita, T., Kamoshita, K., and Nakajima, M. Mechanism of inhibition reaction of acetylcholinesterase by phenyl *N*-methylcarbamates. Pestic. Biochem. Physiol. 7: 107–121 (1977).
16. Yukawa, Y., and Tsuno, Y. Resonance effect in Hammett relationship. II. Sigma constants in electrophilic reactions and their intercorrelation. Bull. Chem. Soc. Japan 32: 965–971 (1959).
17. Nishioka, T., Fujita, T., Kitamura, K., and Nakajima, M. The *ortho* effect in hydrolysis of phenyl esters. J. Org. Chem. 40: 2520–2525 (1975).
18. Fujita, T., and Nishioka, T. The analysis of the *ortho* effect. In: Progress in Physical Organic Chemistry, Vol. 12 (R. W. Taft, Ed.), John Wiley, New York, 1976, pp. 49–89.
19. Swain, C. G., and Lupton, E. C. Field and resonance components of substituent effects. J. Am. Chem. Soc. 90: 4328–4337 (1968).
20. Kamoshita, K., Ohno, I., Fujita, T., Nishioka, T., and Nakajima, M. Quantitative structure-activity relationships of phenyl *N*-methylcarbamates against house fly and its acetylcholinesterase. Pestic. Biochem. Physiol. 11: 83–103 (1979).
21. Kuhr, R. J. Metabolism of carbamate insecticide chemicals in plants and insects. J. Agr. Food Chem. 18: 1023–1050 (1970).
22. Fujita, T. The *ortho* effect in quantitative structure–activity correlations. Anal. Chim. Acta 133: 667–676 (1981).
23. Jaffe, H. H. A reexamination of the Hammett equation. Chem. Rev. 53: 191–261 (1953).
24. Narahashi, T. Effects of insecticides on excitable tissues. In: Advances in Insect Physiology, Vol. 8 (J. W. L. Beament, J. E. Treherne and V. B. Wigglesworth, Eds.), Academic Press, London–New York, 1971, pp. 1–93.
25. Holan, G. New halocyclopropane insecticides and the mode of action of DDT. Nature 221: 1025–1029 (1969).
26. Holan, G., O'Keefe, D. F., Virgona, C., and Walser, R. Structural and biological link between pyrethroids and DDT in new insecticides. Nature 272: 734–736 (1978).
27. Ohno, N., Fujimoto, K., Okuno, Y., Mizutani, T., Hirano, M., Itaya, N., Honda, T., and Yoshioka, H. 2-Arylalkanoates, a new group of synthetic pyrethroid esters not containing cyclopropanecarboxylates. Pestic. Sci. 7: 241–246 (1976).
28. Wooley, D. E. Neurotoxicity of DDT and possible mechanisms of action. In: Mechanisms of Actions of Neurotoxic Substances, (K. Prasad and A. Vernadakis, Eds.), Raven Press, New York, 1982, pp. 95–141.
29. Casida, J. E., Gammon, D. W., Glickman, A. H., and Lawrence, L. J. Mechanisms of selective action of pyrethroid insecticides. In: Annual Review of Pharmacology and Toxicology, Vol. 23 (R. George, R. Okun, and A. K. Cho, Eds.), Annual Reviews Inc., Palo Alto, 1983, pp. 413–438.
30. Nakagawa, S., Okajima, N., Kitahaba, T., Nishimura, K., Fujita, T., and Nakajima, M. Quantitative structure-activity studies of substituted benzyl chrysanthemates. 1. Correlations between symptomatic and neurophysiological activites against American cockroaches. Pestic. Biochem. Physiol. 17: 243–258 (1982).
31. Nakagawa, S., Okajima, N., Nishimura, K., Fujita, T., and Nakajima, M. Quantitative structure-activity studies of substituted benzyl chrysanthemates. 2. Physicochemical substituent effects and neurophysiological and symptomatic activities against American cockroaches. Pestic. Biochem. Physiol. 17: 259–270 (1982).
32. Elliott, M. The relationship between the structure and the activity of pyrethroids. Bull. WHO 44: 315–324 (1970)
33. Nishimura, K., and Fujita, T. Quantitative structure-activity relationships of DDT and its related compounds. J. Pestic. Sci. 8: 69–80 (1983).
34. Holan, G. Mode of action of DDT—new aryl-alicyclic and heterocyclic insecticides. In: Environmental Quality and Safety, Suppl. Vol. III (F. Coulson and F. Korte, Eds.), Georg Thieme Publishers, Stuttgart, 1975 pp. 359–364.
35. Henrick, C. A., Staal, G. B., and Siddall, J. B. Alkyl 3,7,11-trimethyl-2,4-dodecadienoates, a new class of potent insect growth

regulators with juvenile hormone activity. J. Agr. Food Chem. 21: 354–359 (1973).
36. Pallos, F. M., Letchworth, P. E., and Menn, J. J. Novel nonterpenoid insect growth regulators. J. Agr. Food Chem. 24: 218–221 (1976).
37. DeMilo, A. B., and Redfern, R. E. New insect juvenile hormone mimics: aromatic shiff bases and related compounds against the large milkweed bug and yellow mealworm. J. Agr. Food Chem. 27: 760–762 (1979).
38. Henrick, C. A., Willy, W. E., and Staal, G. B. Insect juvenile hormone activity of alkyl (2E,4E)-3,7,11-trimethyl-2,4-dodecadienoates. Variations in the ester function and in the carbon chain. J. Agr. Food Chem. 24: 207–218 (1976).
39. Nakayama, A., Iwamura, H., and Fujita, T. Quantitative structure-activity relationship of insect juvenile hormone mimetic compounds. J. Med. CHem. 27: 1493–1502 (1984).
40. Shantz, E. M., and Steward, F. C. The identification of compound A from coconut milk as 1,3-diphenylurea. J. Am. Chem. Soc. 77: 6351–6353 (1955).
41. Iwamura, H., Fujita, T., Koyama, S., Koshimizu, K., and Kumazawa, Z. Quantitative structure-activity relationship of cytokinin-active adenine and urea derivatives. Phytochemistry 19: 1309–1319 (1980).
42. Bruce, M. I., and Zwar, J. A. Cytokinin activity of some substituted ureas and thioureas. Proc. Roy. Soc. B. 165: 245–265 (1966).
43. Okamoto, T., Shudo, K., and Isogai, Y. Structural and biological links between urea and purine cytokinins. In: Pesticide Chemistry, Vol. 1 (P. Doyle and T. Fujita, Eds.), Pergamon Press, Oxford, 1983, pp. 333–338.
44. Skoog, F., Schmitz, R. Y., Bock, R. Y., and Hecht, S. M. Cytokinin antagonists: Synthesis and physiological effects of 7-substituted 3-methylpyrazolo[4,3-d]pyrimidines. Phytochemistry 12: 25–37 (1973).
45. Iwamura, H., Ito, T., Kumazawa, Z., and Ogawa, Y. Synthesis and anticytokinin activity of 4-substituted-7-(β-*D*-ribofuranosyl)pyrrolo[2,3-d]pyrimidines. Phytochemistry 14: 2317–2321 (1975).
46. Skoog, F., Schmitz, R. Y., Hecht, S. M., and Frye, R. B. Anticytokinin activity of substituted pyrrolo[2,3-d]pyrimidines. Proc. Natl. Acad. Sci. (U.S.) 72: 3508–3512 (1975).
47. Iwamura, H., Masuda, N., Koshimizu, K., and Matsubara, S. Cytokinin-agonistic and antagonistic activities of 4-substituted 2-methylpyrrolo[2,3-d]pyrimidines, 7-deaza analogs of cytokinin-active adenine derivatives. Phytochemistry 18: 217–222 (1979).
48. Iwamura, H., Murakami, S., Koga, J., Matsubara, S., and Koshimizu, K. Quantitative analysis of anticytokinin activity of 4-substituted-2-methylthiopyrido[4,3-d]pyrimidines. Phytochemistry 18: 1265–1268 (1979).
49. Lineweaver, H., and Burk, D. The determination of enzyme dissociation constants. J. Am. Chem. Soc. 56: 658–666 (1934).
50. Iwamura, H., Masuda, N., Koshimizu, K., and Matsubara, S. Quantitative aspects of the receptor binding of cytokinin agonists and antagonists. J. Med. Chem. 26: 838–844 (1983).
51. Cramer, R. D. A. QSAR success story. Chemtech. 1980: 744–747.
52. Unger, S. H. Consequences of the Hansch paradigm. In: Drug Design, Vol. 9 (E. J. Ariëns, Ed.), Academic Press, New York, 1980, pp. 48–121.
53. Martin, Y. C. A practitioner's perspective of the role of quantitative structure-activity analysis in medicinal chemistry. J. Med. Chem. 24: 229–237 (1981).
54. Wooldridge, K. R. H. Antiallergic purinones: a successful application of QSAR. In: Drugs Affecting the Respiratory System (D. L. Temple, Ed.), American Chemical Society, Washington, D. C., 1980, pp. 117–123.
55. Fujita, T. The role of QSAR in drug design. In: Drug Design: Fact or Fantasy (G. Jolles and K. R. H. Wooldridge, Eds.), Academic Press, London, 1983, pp. 19–33.
56. Lien, E. J., and Hansch, C. Structure-activity correlations of antifungal agents: a survey. In: Biological Correlations—The Hansch Approach, Advances in Chemistry Series Vol. 114 (R. F. Gould, Ed.), American Chemical Society, Washington, DC, 1972, pp. 115–182.
57. Hansch, C. Theoretical considerations of the structure-activity relationship in photosynthesis inhibitors. In: Progress in Photosynthesis Research, Vol. 3 (H. Metzner, Ed.), International Union of Biological Sciences, Tübingen, 1969, pp. 1685–1692.
58. Bysshe, S. E. Bioconcentration factor in aquatic organisms. In: Handbook of Chemical Property Estimation Methods (W. J. Lyman, W. F. Reehl and D. H. Rosenblatt, Eds.), McGraw-Hill, New York, 1982, pp. 5-1–5-30.